Interplay between fast ions and turbulence in magnetic fusion plasmas

R. Dumont[1], D. Zarzoso[1,2], Y. Sarazin[1], X. Garbet[1], A. Strugarek[3,1], J. Abiteboul[1,2], T. Cartier-Michaud[1], G. Dif-Pradalier[1], Ph. Ghendrih[1], J.-B. Girardo[1], V. Grandgirard[1], G. Latu[1], C. Passeron[1] and O. Thomine[1].

[1] CEA, IRFM, F-13108 Saint-Paul-lez-Durance, France.
[2] Max-Planck-Institut fr Plasmaphysik, EURATOM Association, Garching, Germany.
[3] DSM/IRFU, CEA/Saclay, Gif-sur-Yvette, France.

Abstract. Evidence for the impact of energetic particles (EPs) on turbulence is given in this paper. Firstly, the excitation of electrostatic instabilities in linear gyrokinetic simulations performed with the global GYSELA code by introducing distribution functions typical of fast ions in tokamak plasmas is presented. The obtained mode is unambiguously characterized as an EGAM, i.e. a Geodesic Acoustic Mode (GAM) excited by EPs. The influence of EGAMs on turbulence and associated transport is then analyzed by implementing a source adapted to the inclusion of fast particle populations in non-linear simulations. This source successfully excites EGAMs in the presence of turbulence, and leads to a drastic reduction of the turbulent transport. However, this reduction is only transient, and is followed by an increase of the turbulent activity, characterized by a complex interaction between the EGAMs and turbulence. In the subsequent steady-state regime, turbulent transport appears to be modulated at the EGAM frequency.

Submitted to: *Plasma Phys. Controlled Fusion*

1. Introduction

Resulting either from the nuclear fusion reactions occurring in the plasma or from external sources such as Ion Cyclotron Resonance Frequency (ICRF) heating and NBI (Neutral Beam Injection) systems, energetic ions are prevalent in modern and future fusion devices. In these experiments, plasma turbulence has also been identified as a major determinant of the energy confinement time, and hence of the discharge performance as a whole. In-depth investigation of the potential interactions between turbulence and energetic particles (EPs) is therefore essential towards reliable performance predictions in next-step fusion reactors.

The direct impact of turbulence on EPs has been found to be limited[1]. The influence of EPs on turbulence, on the other hand, has received relatively little attention, so far. The possibility of controlling, to some extent, the creation and features of the fast ion populations opens the possibility of a potential action on an intrinsically self-regulated system involving turbulence, mean flows, zonal flows[2] and also higher frequency phenomena such as Geodesic Acoustic Modes (GAMs)[3]. Although the latter have an efficiency presumably smaller than stationary or low frequency flow shear generation mechanisms[4], they have been shown to play a central role in the L-H transition, which is believed to involve the same actors in the plasma edge[5].

The reason why GAMs are only observed in the plasma edge, however, is because they are subject to strong Landau damping and therefore cannot impact core turbulence in a stationary fashion. The possibility of overcoming this limitation by exciting similar modes with fast particles therefore represents an appealing prospect. In this case, the mode is usually referred to as an EGAM, and has been predicted theoretically[6, 7] and unambiguously observed in experiments[8, 9]. Recently, detailed numerical studies of the EGAMs properties[10] and their influence on turbulence[11] have been conducted in the framework of gyrokinetic simulations. Another advantage of EGAMs is that unlike GAMs which are non-linearly generated by the turbulence itself, the energetic particle sources can be tuned to some extent, opening the possibility of turbulence control in the plasma core.

2. EGAMs in gyrokinetic simulations

In this paper, we present flux-driven simulations performed with the GYSELA code[12, 13]. The standard gyrokinetic equation for the full-f ion gyro-centre distribution function F can be written as

$$\frac{\partial F}{\partial t} + \mathbf{v} \cdot \nabla F + \dot{v}_{\parallel} \frac{\partial F}{\partial v_{\parallel}} = \mathcal{C}(F) + S_{th} + S_{EP}, \tag{1}$$

where $\mathcal{C}(F)$ represents the collision operator whose features are extensively discussed in Ref. [13]. S_{th} is the thermal source and S_{EP} is the source aimed at introducing fast energetic particles in the simulations. The electrostatic limit is considered, and electrons are assumed adiabatic. The magnetic topology consists of concentric toroidal magnetic flux surfaces with circular poloidal cross-sections. In this work, the time is normalized with respect to $\omega_c^{-1} \equiv m_i/eB_0$ with e the elementary charge, m_i the ion mass and B_0 the confining magnetic field on axis. Temperatures (resp. velocities) are normalized to the bulk temperature T_i (resp. bulk thermal velocity v_{th}).

In order to check the possibility of observing EP instabilities in gyrokinetic simulations, and also characterize them as extensively as possible, linear calculations

without turbulence have been performed. This has been done by setting $\mathcal{C}(F) + S_{th} + S_{EP} = 0$ in Eq. 1 and assuming flat equilibrium profiles to make sure that ITG turbulence is not excited. In this case, the initial equilibrium distribution function is written as $F(t=0) \equiv F_{eq}(1 + \varepsilon(r)\sin(\theta))$ with θ the poloidal angle and $\varepsilon(r)$ the amplitude of the initial perturbation. F_{eq} is made of the sum of a thermal and a fast particle contribution, i.e. $F_{eq} \equiv F_{eq,i} + F_{eq,h}$ with $F_{eq,i}$ a Maxwellian characterized by equilibrium density n_i and temperature T_i. $F_{eq,h}$ is a bump-on-tail distribution, which is written as

$$F_{eq,h} \equiv F_{M,h} \exp\left(-\frac{v_\parallel^2}{2T_h}\right) \cosh\left(\frac{v_0 v_\parallel}{T_h}\right), \tag{2}$$

where $F_{M,h}$ is a Maxwellian characterized by density n_h and temperature T_h. $v_\parallel$ is the parallel velocity and v_0 is representative of the excited parallel velocity. Locally, this distribution function may exhibit a positive slope with respect to energy, i.e. $\partial F/\partial E > 0$, which is a necessary condition for the mode excitation.

It has been predicted that EGAMs are unstable only when the fast ion density exceeds a given threshold[6, 10]. A scan in the energetic ion density has therefore been conducted with GYSELA by varying the fast ion concentration (n_h) in the model distribution function (Eq. 2). The other parameters are $T_h = 1$ and $v_0 = 4$. From the calculation result, $\Im(\phi_{10})$, the steady-state oscillation of the $(m,n) = (1,0)$ component of the electrostatic potential ϕ representative of the EGAM, is Fourier analyzed in time. This yields the mode frequency ω. The linear growth rate, γ, is deduced from the time evolution. The scan results are shown in Fig. 1(a).

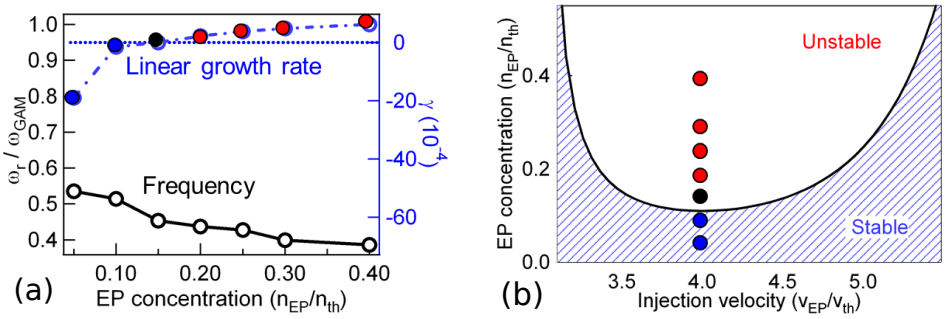

Figure 1. (a) Normalized frequency (left y-axis) and linear damping rate (right y-axis) of the ϕ_{10} oscillation versus fast ion concentration. (b) Dependence of the linear threshold versus injection velocity and fast particle concentration. The points corresponding to $v_0 = 4$ and shown in (a) are reported.

In the presence of energetic particles, an oscillation in ϕ_{10} is systematically observed at $\omega \sim 0.5\omega_{GAM}$, including below the linear threshold. It is worthwhile mentionning that a peak at $\omega = \omega_{EGAM}$ is also appearent on other Fourier components as a result of mode coupling in toroidal geometry, but it is systematically most pronounced on $\Im(\phi_{10})$, viz. the up-down asymmetric part of ϕ, as expected for an EGAM. The frequency (resp. growth rate) decreases (resp. increases) with the fast ion concentration. These results are consistent with theoretical predictions[6] regarding EGAMs. In order to further characterize the observed oscillation, the obtained results are compared to a theoretical model derived in Ref. [10]. In this reference, the stability diagrams of EGAMs for two model distribution functions and various parameters are

established. In Fig. 1, the stability diagram corresponding to the distribution function given by Eq. 2 with $T_h = 1$ is shown. The simulation points appearing in Fig. 1(a) with $v_0 = 4$, are reported on this diagram and show that the threshold observed in numerical simulations is in good agreement with the theoretical prediction. These results point to the successful excitation of EGAMs by fast ions in GYSELA.

3. Turbulent simulations in the presence of energetic particles

To analyze the interaction between fast ions and turbulence mediated by EGAMs, it is necessary to excite the mode in the ambient turbulence. Since GYSELA simulations are flux-driven and account for collisions, the procedure discussed previously for linear simulations can not be applied. Indeed, any initial distribution function will rapidly thermalize and the EGAMs drive ($\partial F/\partial E > 0$) will vanish as soon as the system relaxes towards equilibrium. A source aimed at creating fast particles has therefore been implemented in GYSELA. This bears some resemblance to actual experiments in which ICRF sources or neutral beam injectors are used to heat the plasma by injecting energy. It is worthwhile mentioning that these sources also inject other fluid moments as well such as momentum or vorticity into the discharge. In the framework of the present study, however, it is desirable to separate the various effects and the source is therefore designed so as to inject only energy in the parallel direction. This is done by using the following form[15] for S_{EP} (see Eq. 1)

$$S_{EP} = S_0(r,t)\{\mathcal{S}_\parallel(\bar{v}_\parallel + \bar{v}_0) + \mathcal{S}_\parallel(\bar{v}_\parallel - \bar{v}_0)\}e^{-\bar{\mu}B}. \quad (3)$$

In the previous expression, $\bar{v}_0 \equiv v_0/\sqrt{2T_{\parallel,s}}$ is the parallel injection velocity and $\bar{v}_\parallel \equiv v_\parallel/\sqrt{2T_{\parallel,s}}$. Both are normalized with respect to a parallel temperature $T_{\parallel,s}$, characterizing the source. $\bar{\mu}$ is the magnetic moment, normalized to the transverse temperature of the source $T_{\perp,s}$, which is set to 1 in the present simulations. The symmetry of this form with respect to $v_\parallel$ ensures that the constraint of zero momentum injection is fulfilled. In Fig. 2(a), a schematic representation of the source effect is shown versus the parallel energy for $\bar{v}_0 = 2$ and $T_{\parallel,s} = 0.5$. The source has the effect of pumping particles around $\bar{v}_0$ and either increasing or decreasing their parallel velocity to maintain a constant density.

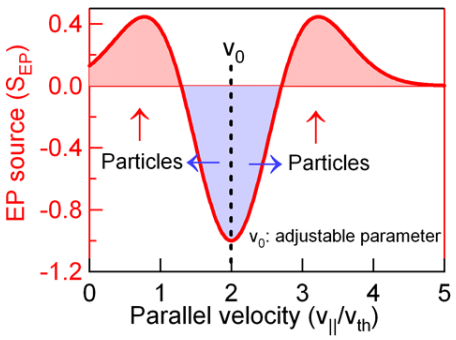

Figure 2. Schematic representation of the source of energetic particle versus parallel velocity for $\bar{v}_0 = 2$ and $\bar{T}_{\parallel,s} = 0.5$.

A difficulty arising when assessing the effect of EGAMs on turbulence is to clearly isolate this effect when comparing simulations with or without the modes. A

possibility would be to simply set S_{EP} to zero in a reference simulation, and to a finite value in a simulation with EGAMs, but the obtained results would differ in the total injected power. Consequently, the ITG turbulence would have differing characteristics regardless of EGAMs, and quantitative assessment of the effect of the mode would be quite complicated. The procedure which has been employed in the present study is thus to compare two simulations with the fast particle source switched on, but with $\bar{v}_0 = 0$, $\bar{T}_{\parallel,s} = 1$ on the one hand and $\bar{v}_0 = 2$, $\bar{T}_{\parallel,s} = 0.5$ on the other hand. These conditions ensure that the total injected power is rigorously the same in both cases. However, in the first one, the source does not induce a positive slope in the distribution function. As expected, no EGAMs are observed in the simulation. Although the EP source is used in both situations, the first case ($\bar{v}_0 = 0$) will hereinafter be referred to as "without energetic particles", whereas the second case ($\bar{v}_0 = 2$) will be deemed "with energetic particles".

Two such simulations are compared, using the same thermal source with an injected power of 4MW. The collisionality is $\nu_\star = 0.02$ (banana regime), the safety factor q profile is parabolic with a relatively low magnetic shear ($0 < s < 0.4$) and such that $q \approx 2.7$ at mid-radius. The normalized Larmor radius is $\rho_\star = 1/150$. The initial density and temperature profiles are characterized by $R/L_n = 2.2$ and $R/L_T = 6.5$ respectively, with R the major radius, L_n and L_T the gradient lengths. Since there is no particle transport, L_n remains constant. Both simulations are strictly identical in the time window $t < t_{\text{init}}$, during which only the thermal source is used. At $t = t_{\text{init}}$, turbulence has reached a statistical steady state, and the fast particle source is switched on, leading to an additional input power of 2MW. The radial profiles of the thermal and energetic particle sources are represented in Fig. 3. Whereas the thermal source is peaked and localized only in the inner radial region, the energetic particle source spreads over an extended region to minimize its direct impact on the temperature profile. In the same figure are plotted the initial temperature profile and the diffusive boundary regions, in which articifial diffusion and increased collisionality are introduced in order to damp turbulence and regularize the distribution function in the vicinity of the radial simulation boundaries[13].

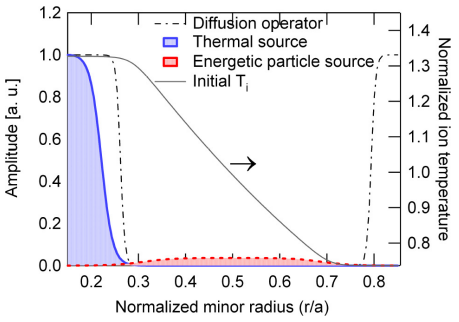

Figure 3. Radial profiles of the the thermal source (shadowed blue area), the energetic particle source (shadowed red area), the ion temperature (solid black line) and the diffusive regions in the boundary of the simulation box.

Firstly, the ability of the EP source at inverting the distribution function, and potentially excite EGAMs, is checked by plotting $\partial F/\partial v_\parallel$ at the resonant velocity $v_{\parallel,res} = qR\omega_{GAM}$ in Fig. 4.

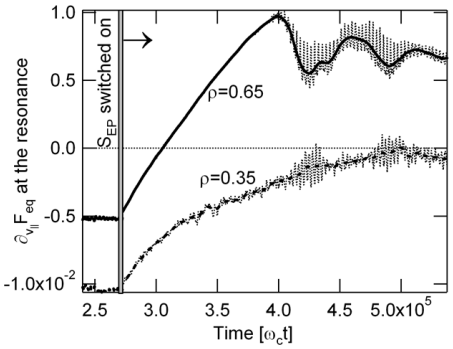

Figure 4. Time evolution of the derivative of distribution function at the EGAM resonant velocity.

We observe that after the EP source switch-on, the distribution function is reversed in the outer region $\rho \gtrsim 0.5$. In order to determine whether EGAMs are excited, we compare the frequency spectrum of $\Im(\phi_{1,0})$ in both situations. The result is shown in Fig. 5. In the presence of fast particles, a clear peak is observed at $\omega \approx 0.4\omega_{GAM}$, corresponding to the EGAM frequency ω_{EGAM} already observed in linear simulations. A secondary, lower, peak is observed around the harmonic frequency $\omega = 2\omega_{EGAM}$, which we attribute to the resulting non-linear wave-wave interaction. Another observation is that the EGAM frequency is clearly embedded in the turbulent spectrum. This has the consequence that the interaction between EGAMs and turbulence is potentially strong, but also precludes the use of simple models based on scale separation assumptions to investigate it in details. Interestingly, we note in Fig. 4 that the distribution function slope remains negative at inner radii ($\rho = 0.35$ in the figure) but EGAMs are nevertheless observed at these positions, despite the fact that they are linearly stable. This underlines the needs for a global code, with no separation between equilibrium and fluctuating quantities, to study these phenomena. Regular GAMs are also systematically observed in the initial phase of the simulations but they are damped as discussed in Ref. [14] and therefore are not likely to play any significant role in regulating the turbulence in the plasma core.

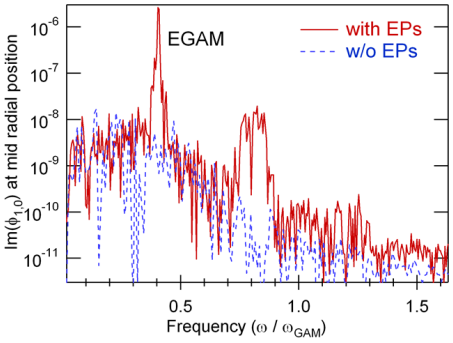

Figure 5. Amplitude of $\Im(\phi_{10})$ in the presence (red line) and in the absence of fast particles (blue, dotted line) (see Ref. [11]).

A relevant quantity to characterize the turbulent transport is the thermal diffusivity $\chi_{E\times B}$, which is governed by fluctuations of the radial component of the $\mathbf{E}\times\mathbf{B}$ drift velocity v_{Er}

$$\chi_{\mathrm{E\times B}} \approx -\frac{Q_{E\times B}}{n_i \nabla_r T}, \tag{4}$$

where $Q_{E\times B} = \langle v_{Er} p\rangle$ is the radial heat flux associated to v_{Er} and p is the pressure. These quantities are directly available from the simulations.

In Fig. 6, $\chi_{E\times B}$ is shown versus time and minor radius. Three phases, denoted A, B and C are visible: (A) the EP source is applied to an established steady-state turbulent regime, (B) a transport barrier develops and (C) EGAMs and turbulence coexist and interact with each other in a non-trivial fashion.

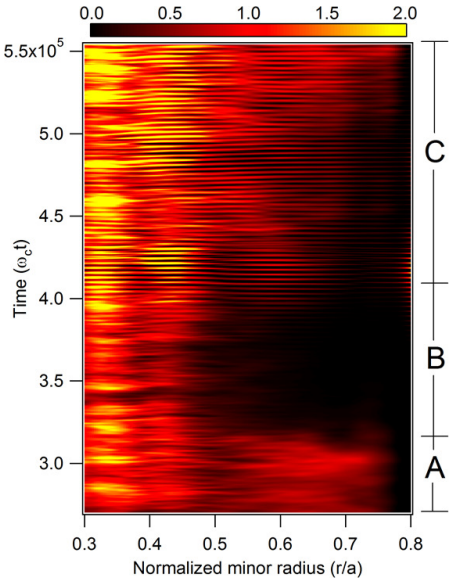

Figure 6. 2D representation of the $\mathbf{E}\times\mathbf{B}$ heat diffusivity versus normalized radius and time[11], showing the three phases discussed in the article.

In order to gain more insight into the turbulent transport in these simulations, Fig. 7 shows the evolution of $|\delta\phi|^2$ and $\chi_{E\times B}$ versus time, averaged over region $0.5 < \rho < 0.8$. In order to separate the effect of EGAMs and turbulence, the contribution of axisymmetric modes ($n = 0$) and non-axisymmetric modes ($n \neq 0$) are shown separately.

Fig. 7 shows that EGAMs only appear near the end of phase B. In phase C, they are observed to coexist with non-axisymmetric contributions to the electrostatic potential with similar magnitudes. After the EP source has been switched on, the turbulent diffusivity is found to drop substantially, as a consequence of a large reduction of the ITG activity. This is attributed to the depletion of the resonant particles driving the ITG instability, directly caused by the source when $\bar{v}_0 = 2$. Whether this effect is coincidental and results from this particular choice of simulation parameters or is the signature of a more general mechanism related to external heating of fusion plasmas remains to be firmly established. We also note that other mechanisms

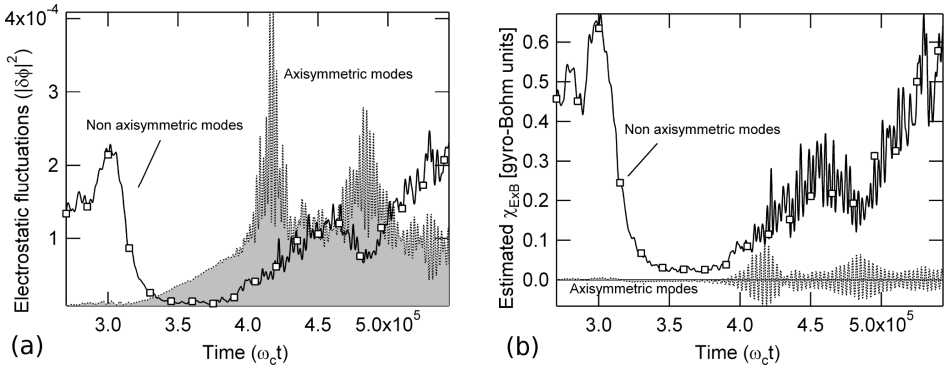

Figure 7. Contribution of $n = 0$ and $n \neq 0$ modes to the time evolution of (a) the electrostatic potential fluctuations, (b) the turbulent diffusivity in the presence of energetic particles.

such as a direct effect of the source anisotropy can not be excluded[16]. In any case, this drastic reduction of the turbulent transport is only transient and $\chi_{E\times B}$ increases to reach a level comparable to the turbulent diffusivity prior to the application of the EP source. We note, however, that the contribution of $n = 0$ modes to the heat diffusivity remains negligible during the whole simulation, indicating that the transport increase is not directly caused by the EGAMs.

Interestingly, in phase C, a spectral analysis shows that the turbulent diffusivity itself is modulated at the EGAM frequency, suggesting that the net increase of diffusivity and the excitation of EGAMs are correlated. In this phase, E_r, the radial electric field exhibits large oscillations at $\omega = \omega_{EGAM}$. The resulting electric shear does not suppress turbulence. Instead, $\chi_{E\times B}$ itself exhibits oscillations at the EGAM frequency and its time-averaged value increases only when EGAMs are excited. This reveals a strong interaction between the energetic particles and the turbulence, via the excitation of EGAMs.

The complex interaction between turbulence and EGAMs is further illustrated in Fig. 8, where the evolution of the oscillating part of R/L_T, defined as $R/L_T - \langle R/L_T \rangle_t$ with $\langle\cdot\rangle_t$ the time average, is plotted for two different time windows. This figure corresponds to the appearance of EGAMs at the end of the phase B (bottom panel) and to the phase where turbulence and EGAMs coexist, during phase C (top panel). When a transport barrier is observed, the inner region exhibits avalanche-like behavior, with fronts propagating outwards and vanishing at $\rho \approx 0.5$. In the same figure, EGAMs manifest themselves as static oscillations in the outer region, characterized by horizontal traces. In phase C, we see that there is not a single propagation velocity, i.e. both outwards propagating fronts and static oscillations coexist and the outer radial region is also characterized by an avalanche-like behavior. As a result, energy appears to flow from the plasma core to outer regions along radially elongated structures. Mechanisms underlying this phenomenon are still being studied. One possibility is that the EGAM transfers energy to turbulent modes via a decay parametric process. In that process, the EGAM is the pump wave, whereas two ITG modes, with identical toroidal and poloidal wave numbers but frequencies shifted by the EGAM frequency, are the daughter waves. The reverse process, i.e. the parametric excitation of a GAM by a pump drift wave via a second drift wave, has been investigated by F. Zonca

and L. Chen [17]. This may lead to a locking of the avalanches and the electrostatic oscillations[18].

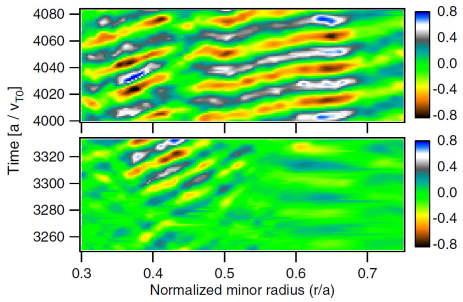

Figure 8. A comparison of the oscillating part of R/L_T in a simulation with fast particles[11] at the end of phase B (bottom) and during phase C (top).

4. Summary

A clear impact of energetic particles (EPs) on turbulence has been observed in gyrokinetic simulations performed with the global GYSELA. By introducing distribution functions typical of fast ions in the absence of turbulence, a mode unambiguously characterized as an EGAM has been observed for parameters consistent with theoretical predictions. The influence of EGAMs on turbulence and associated transport has subsequently been studied using an ad-hoc source introducing fast particles in non-linear simulations. This source firstly leads to a drastic reduction of the turbulent transport. However, this reduction is only transient, and is followed by an increase of the turbulent activity, characterized by an apparent locking between the EGAMs and avalanches. More generally, this study shows that a radial electric shear oscillating at a frequency $\omega \sim \omega_{\mathrm{ITG}}$ is unlikely to be an efficient way to suppress turbulence. Neverthless, future simulations will explore a wider range of source conditions in order to further approach experimentally relevant conditions corresponding to either NBI or ICRF heating in a reactor.

Acknowledgments

This work was granted access to the HPC resources of CINES under the allocation 2012052224 made by GENCI (Grand Equipement National de Calcul Intensif). This work was supported by EURATOM and carried out within the framework of the European Fusion Development Agreement. The views and opinions expressed herein do not necessarily reflect those of the European Commission.

References

[1] W. Zhang, Z. Lin and L. Chen, Phys. Rev. Lett. **101**, 095001 (2008).
[2] P. H. Diamond, S.-I. Itoh, K. Itoh, and T.-S. Hahm, Plasma Phys. Control. Fusion **47**, R35 (2005).
[3] N. Winsor, J. L. Johnson, and J. M. Dawson, Phys. Fluids **11**, 2448 (1968).
[4] T. S. Hahm, Phys. Plasmas **1**, 2940 (1994).

[5] G. D. Conway, C. Angioni, F. Ryter, P. Sauter, and J. Vicente, Phys. Rev. Lett. **106**, 065001 (2011).
[6] G. Y. Fu, Phys. Rev. Lett. **101**, 185002 (2008).
[7] Z. Qiu, F. Zonca, and L. Chen, Plasma Phys. Controlled Fusion **52**, 095003 (2010).
[8] C. J. Boswell, H. L. Berk, C. N. Borba, T. Johnson, S. D. Pinches, and S. E. Sharapov, Phys. Lett. A **358** 154 (2006).
[9] R. Nazikian, G. Y. Fu, M. E. Austin, H. L. Berk, R. V. Budny, N. N. Gorelenkov, W. W. Heidbrink, C. T. Holcomb, G. J. Kramer, G. R. McKee, M. A. Makowski, W. M. Solomon, M. Shafer, E. J. Strait, and M. A. Van Zeeland, Phys. Rev. Lett. **101** 185001 (2008).
[10] D. Zarzoso, X. Garbet, Y. Sarazin, R. Dumont, and V. Grandgirard, Phys. Plasmas **19**, 022102 (2012).
[11] D. Zarzoso, Y. Sarazin, X. Garbet, R. Dumont, A. Strugarek, J. Abiteboul, T. Cartier-Michaud, G. Dif-Pradalier, Ph. Ghendrih, V. Grandgirard, G. Latu, C. Passeron, and O. Thomine, Phys. Rev. Lett. **104**, 185003 (2013).
[12] V. Grandgirard, Y. Sarazin, X. Garbet, G. Dif-Pradalier, Ph. Ghendrih, N. Crouseilles, G. Latu, E. Sonnendrücker, N. Besse, P. Bertrand, Commun. Nonlinear Sci.and Numer. Simul. **13**, 81 (2008)
[13] Y. Sarazin, V. Grandgirard, J. Abiteboul, S. Allfrey, X. Garbet, Ph. Ghendrih, G. Latu, A. Strugarek and G. Dif-Pradalier, Nucl. Fusion **50** 054004 (2010).
[14] G. Dif-Pradalier, V. Grandgirard, Y. Sarazin, X. Garbet, P. Ghendrih, and P. Angelino, Phys. Plasmas **15**, 042315 (2008).
[15] Y. Sarazin, V. Grandgirard, J. Abiteboul, S. Allfrey, X. Garbet, Ph. Ghendrih, G. Latu, A. Strugarek, G. Dif-Pradalier, P. H. Diamond, S. Ku, C. S. Chang, B. F. McMillan, T. M. Tran, L. Villard, S. Jolliet, A. Bottino, and P. Angelino, Nucl. Fusion **51** 103023 (2011).
[16] J. Y. Kim, W. Horton, D. I. Choi, S. Migliuolo, and B. Coppi, Phys. Fluids B **4**, 152 (1992);
[17] F. Zonca and L. Chen EPL **83**, 35001 (2008)
[18] F. Zonca, *Private communication.*